Regulatory Toxicology and Pharmacology 65 (2013) 135–146

Contents lists available at SciVerse ScienceDirect

Regulatory Toxicology and Pharmacology

journal homepage: www.elsevier.com/locate/yrtph

# Nickel release and surface characteristics of fine powders of nickel metal and nickel oxide in media of relevance for inhalation and dermal contact

Neda Mazinanian, Yolanda Hedberg, Inger Odnevall Wallinder *

*KTH Royal Institute of Technology, Division of Surface and Corrosion Science, School of Chemical Science and Engineering, 100 44 Stockholm, Sweden*

ARTICLE INFO

*Article history:*
Received 12 June 2012
Available online 8 November 2012

*Keywords:*
Nickel
Nickel oxide
Particles
Surface composition
Metal release
Dissolution
Complexation

ABSTRACT

Differences in surface oxide characteristics and extent of nickel release have been investigated in two thoroughly characterized micron-sized (mainly <4 μm) nickel metal powders and a nickel oxide bulk powder when immersed in two different synthetic fluids, artificial sweat (ASW-pH 6.5) and artificial lysosomal fluid (ALF-pH 4.5) for time periods up to 24 h. The investigation shows significantly more nickel released from the nickel metal powders (<88%) compared to the NiO powder (<0.1%), attributed to differences in surface properties. Significantly more nickel was released from the nickel metal powder with a thin surface oxide predominantly composed of non-stoichiometric nickel oxide (probably $Ni_2O_3$), compared to the release from the nickel metal powder with a thicker surface oxide predominantly composed of NiO and to a lesser extent $Ni_2O_3$ (88% and 25% release after 24 h in ALF, respectively). Significantly lower amounts of nickel were released from the nickel metal powders in ASW (2.2% and <1%, respectively). The importance of particle and surface characteristics for any reliable risk assessment is discussed, and generated data compared with literature findings on bioaccessibility (released fraction) of nickel from powders of nickel metal and nickel oxide, and massive forms of nickel metal and nickel-containing alloys.



## 1. Introduction

As it is often the case for metals, the physicochemical properties (particle size and size distribution, agglomeration, surface properties) of different nickel-containing substances will influence their toxicological behavior. Water soluble compounds like nickel sulfate or nickel chloride are usually expected to have different toxicities compared to sparingly soluble nickel compounds (Henderson et al., 2012). For those nickel-containing substances that release limited amounts of nickel in aqueous solutions, the surface properties may be decisive to deliver nickel ions at target cellular sites and to be absorbed and/or excreted. The current work hence focuses to assess differences in physicochemical surface properties (i.e., thickness, crystallinity and composition of surface oxides) between samples of nickel metal powders (nickel in elemental state of oxidation) which are naturally covered by a thin nickel oxide (shell) and nickel(II) oxide (green) powders.

Nickel metal is currently classified for human health endpoints: as a skin sensitizer (Category 1, "may cause an allergic skin reaction"), for causing specific target organ toxicity, STOT RE 1 (STOT Repeated Exposure 1: H372: "causes damage to organs through prolonged or repeated exposure"; "route of exposure: inhalation"), and as a suspected carcinogen (Category 2, "suspected of causing cancer") (EC, 2009), while nickel oxide (NiO) is classified as Category 1Ai carcinogen ("may cause cancer by inhalation"), STOT RE 1, and skin sensitizer (Category 1) (EC, 2009).

Human exposure to nickel metal and/or nickel oxide may occur via the main exposure routes (inhalation, ingestion or dermal contact) at occupational settings. Exposure to nickel metal or nickel-containing alloys can also occur via coins (Kasprzak et al., 2003; Lidén and Carter, 2001; Lidén et al., 2008). Cutaneous nickel absorption may result from wearing or handling of jewelries, coins, or utensils fabricated from nickel alloys or nickel coatings (Flint, 1998; Lidén and Carter, 2001; Lidén et al., 2008), although dermal absorption of nickel from nickel metal and Ni-containing alloys is very low (approximately 0.2%, (Hostynek et al., 2001)). Nickel in fly-ash from coal-fired power plants and petroleum, and smoking are examples of sources that may increase the inhaled nickel dose (Sunderman and Oskarsson, 1991; Denkhaus and Salnikow, 2002). Nickel in fly ash is not present as metallic nickel but rather as nickel sulfate and complex Ni oxides (Huggins et al., 2011). Increased incidence of respiratory cancer has been observed among some groups of nickel refinery workers exposed to sulfidic, oxidic and water soluble nickel compounds, e.g. review by Goodman et al. (2011). Only respiratory tumors have been consistently associated with exposure to nickel-containing compounds (Goodman et al., 2011). While the positive association between increased respiratory cancer mortality and overexposures to nickel oxide observed in epidemiological studies was confirmed in animal inhalation

* Corresponding author. Fax: +46 208284.
*E-mail address:* ingero@kth.se (I. Odnevall Wallinder).

0273-2300 
http://dx.doi.org/10.1016/j.yrtph.2012.10.014

studies, both animal and human studies show that nickel metal powders are not expected to increase the risk of respiratory cancer (Goodman et al., 2011; Oller et al., 2008). Prior to 2008, when the classification of nickel metal as a Category 2 carcinogen took place, no animal inhalation carcinogenicity study with nickel metal powder was available.

Skin irritation induced by nickel metal and nickel oxide particles seem to be solely related to released soluble nickel species, such as nickel ions, i.e. the *bioaccessible fraction* (the fraction of the sample that has been released or has been solubilized and available for uptake or absorption by humans). Due to the known relationship between the release of nickel ions and skin sensitization (Flint, 1998; Lidén and Carter, 2001; Lidén et al., 2008; Midander et al., 2007), any nickel-containing articles in direct and prolonged contact with the skin are classified as skin sensitizers when exceeding a release rate of 0.5 μg Ni/cm$^2$/week, as measured by the European Standard reference test method EN 1811 (EN, 2011; EC, 2009). For piercing assemblies, the nickel release limit allowed for the materials to remain in commerce is set to 0.2 μg Ni/cm$^2$/week (EN, 2011). Many investigations have therefore focused on assessing the bioaccessibility of different nickel compounds, alloys, powders and/or massive material in artificial sweat (Hedberg et al., 2010b; Lidén and Carter, 2001; Lidén et al., 2008; Midander et al., 2007). Nickel-induced allergies are the most frequent reasons for contact dermatitis in the industrialized part of the world, affecting 15% of females and a few% of males (Lidén and Carter, 2001). The ability of nickel ions to cause a dermal reaction in sensitized individuals depends on their concentration, the exposed skin area and the exposure duration (Flint, 1998). Generally, a concentration exceeding 1.5 μg Ni chloride per cm$^2$ of skin in an open application is required to elicit dermatitis in sensitized individuals (Menné and Calvin, 1993). However, lower concentrations may also induce an allergic reaction if other irritants or allergens are present in parallel (Pedersen et al., 2004).

Due to non-stoichiometric composition of nickel oxides, their physico-chemical properties (i.e., impurities, oxygen content, crystallinity, phases, and water solubility) are not constant and have therefore yielded considerably variable results in cytotoxicity and carcinogenicity studies (Takahashi et al., 1999). The only reasonably well-characterized surface oxide formed on pure nickel metal at room temperature is NiO (Greenwood and Earnshaw, 1997; Kitakatsu et al., 1998; Mitchell et al., 1976), covered by a nearly saturated layer of hydroxyl groups ($OH^-$) (Kitakatsu et al., 1998). However, claims for the existence of many other oxides ($Ni_2O_3$, $NiO_2$) have been made (Barrientos et al., 2009; Greenwood and Earnshaw, 1997). Green nickel oxide (tested in this study) has a rock-salt stoichiometric structure (face cubic centered) (Greenwood and Earnshaw, 1997), poor solubility, and to some extent lower respiratory toxicity than other nickel compounds when compared by acute or subchronic effects (Oller et al., 1997; Takahashi et al., 1999). A study comparing ten different NiO powders reports significant differences in, e.g., solubility (in water, rat serum, and renal cytosol), phagocytosis, morphological transformation and cytotoxicity, and stimulation of erythropoiesis (Sunderman et al., 1987). From that study it was concluded that a high specific surface area and the presence of Ni(III) were associated with the largest biological effects.

Different physical, chemical, or electrochemical processes or their combinations can induce the release of nickel from nickel metal or nickel oxide. For example, nickel metal can be dissolved via corrosion processes in contrast to nickel oxide, which is in its thermodynamically stable form in oxygen environments. For complexing media such as artificial lysosomal fluid (ALF, pH 4.5), which simulates intracellular inflammatory conditions in lung cells following phagocytosis (de Meringo et al., 1994), adsorption of the complexing agents on the particle surface and subsequent complexation to the metal oxide is important (Hedberg et al., 2011). While dissolution of nickel oxide particles in non-complexing media is mainly due to the proton adsorption (pH), showing increasing dissolution with decreasing pH (Ludwig and Casey, 1996), dissolution is significantly enhanced by complexing agents such as oxalate (Ludwig et al., 1996).

The objective of this study was to investigate differences in particle and surface oxide characteristics and the extent of nickel release from micron-sized (<1–50 μm, mainly <4 μm) nickel metal powders compared with a nickel oxide bulk powder to assess whether these differences could explain differences in reported toxicological behavior of such powders. Bioaccessibility studies have been conducted in synthetic fluids of relevance for the two main exposure routes where the release of nickel ions are important for nickel toxicity including artificial sweat, ASW (skin sensitization) and artificial lysosomal fluid, ALF (respiration). This was accomplished via (i) detailed particle characterization in terms of surface area, particle size distribution, particle morphology, and compositional analysis of the surface oxide, and (ii) the assessment of the amount and kinetics of released nickel from the different powders immersed in ASW, pH 6.5, and ALF, pH 4.5, after four different time periods up to 24 h. Generated release data is compared to in vivo respiratory toxicity and carcinogenicity data on the same or similar samples of nickel metal and nickel oxide powders, powder and massive forms of nickel metal and nickel-containing alloys.

## 2. Materials and methods

### 2.1. Materials

A nickel oxide powder, denoted "NiO (N46)", and two nickel metal powders of different particle size distribution, denoted "Ni (N13)" and "Ni (N36)", were supplied by the Nickel Producers Environmental Research Association (NiPERA). The nickel metal powder sample (N36) used in the animal studies (Oller et al., 2008) was not ground and therefore the powder tested in vitro is the same as the one the animals were exposed to, allowing comparisons between the in vitro and in vivo results to be made.

### 2.2. Particle characterization

#### 2.2.1. BET - specific surface area

The specific surface area per mass (m$^2$/g), BET-analysis (Brunauer–Emmet–Teller method, (Brunauer et al., 1938)) was determined via adsorption of nitrogen at cryogenic condition using a Micromeritics Gemini V instrument. Nitrogen adsorption was measured at five different partial pressures ($p/p_0$ 0.10–0.25). The cross-sectional diameter of nitrogen (0.162 nm$^2$) was used as input parameter. The powders were dried with nitrogen and flushed in a tube for 30 min at 150 °C. The measured mass was adjusted to correspond to an approximate total surface of 1 m$^2$. The results are presented in Table 1.

#### 2.2.2. Particle size distribution

Differences in particle size distribution between the different powders were measured in artificial sweat, ASW, with a relatively

**Table 1**
Measured BET area (m$^2$/g) of the NiO and Ni metal powders, with a standard deviation of less than 1%.

| Powders | BET area |
|---|---|
| NiO (N46) | 0.25 |
| Ni (N13) | 1.05 |
| Ni (N36) | 2.15 |

high ionic strength of 0.11 M (Table 2) and in phosphate buffered saline, PBS, with identical ionic strength as in human blood of 0.15 M containing 8.77 g/L NaCl, 1.28 g/L $Na_2HPO_4$, and 1.36 g/L $KH_2PO_4$, adjusted with 370 μL/L 50% NaOH, pH 7.2–7.4. Low angle laser light scattering (LALLS) was employed using a Malvern Mastersizer 2000 equipment with a Hydro SM dispersion unit. Refractive indexes of NiO (2.180) and water (1.33, since it was the solvent of the test medium) were considered as input parameters at standard operational conditions. Triplicate measurements and duplicate samples were measured (in total six measurements) for each powder. The results are presented as mean values and standard deviations, both in terms of volume mass% and number%.

#### 2.2.3. Particle morphology

Shape and morphology of the powders were investigated by using a field emission gun scanning electron microscope (FEG-SEM, LEO 1530) equipped with a Gemini column (15 kV, 5.5 mm distance).

#### 2.2.4. Compositional analysis of surface oxides

A Horiba HR800 instrument was used for confocal Raman spectroscopy measurements, using a 514 nm laser (no filter), a 500 μm pinhole, an Olympus 10× (0.25 NA) objective and an approximate spot size of 2.5 μm.

X-ray diffraction, XRD, was performed using a D8 equipment from Bruker AXS, with parallel beam arrangement, a Goebbel mirror, a 1.2 mm divergence slit, a long Soller slit on the detector side, a Cu Kα X-ray source and an energy dispersive detector, SolX (Bruker). The goniometer was set up in $\theta$–$\theta$ arrangement with a fixed sample. Measurements were performed between 5° and 100° ($2\theta$) with a step-size of 0.05° and a scan-speed of 5° $min^{-1}$.

Furthermore, chemical analysis of the outmost surface (5–10 nm) of the powders was performed by means of X-ray photoelectron spectroscopy, XPS (UltraDLD spectrometer from Kratos Analytical, Manchester, UK) using a monochromatic Al Kα X-ray source (1486.6 eV) operated at 300 W. The powders were mounted on double adhesive copper tape before being introduced into the UHV chamber. All measurements were performed with an electrostatic lens to reduce peak intensities due to the magnetic properties of the powders. High resolution spectra (20 eV) were acquired for Ni 2p, O1s and C 1s. The elemental peak positions on the binding energy scale provide information about the chemical state. The hydrocarbon peak at 285.0 eV was used as internal standard.

### 2.3. Bioaccessibility studies

Nickel release studies were carried out by immersing a specific particle loading (100 mg/L: 5 mg/50 mL) in Artificial Lysosomal Fluid (ALF) of pH 4.5 at 37 °C and in Artificial Sweat (ASW) of pH 6.5 at 30 °C, both for exposures of 0.5, 2, 6, and 24 h. The loading of 0.1 g/L is recommended by the OECD transformation/dissolution protocol for aquatic acute tests (UN, 2009) and has previously been found to be suitable to avoid extensive particle agglomeration, compared with higher loadings (Hamel et al., 1998; Midander et al., 2006, 2007; Turner, 2011). ALF was used to simulate intracellular inflammatory conditions in lung cells following phagocytosis (de Meringo et al., 1994), relevant to inhalation exposure. Artificial sweat was used to simulate dermal contact according to EN 1811 (EN, 2011), and represents a less aggressive and less acidic solution compared with ALF. Chemical compositions of ALF and ASW are given in Table 2. The pH of ALF was adjusted by using 1.7 mL/L 50% NaOH to pH 4.5 ± 0.05, and for ASW, by using 1 wt.% ammonia solution (to pH 6.5 ± 0.05). ASW was freshly prepared and used within 2 h. All samples were immersed in closed acid-cleaned polymethylpentene (PMP) Nalgene jars (closed) located in a Stuart platform-rocker incubator (37 or 30 °C ± 0.5 °C, 25 cycles/min of bi-linear shaking). In this closed setting, and for the nickel metal samples, dissolved oxygen may be consumed over time by the corrosion reaction if sufficiently rapid, as previously seen for copper (Ullmann, 2008). This set-up of mild bi-linear shaking has previously been found to be advantageous in terms of avoiding particle agglomeration and additional erosion-induced metal release (Midander et al., 2006). Triplicate powder samples and one blank sample, without any powder, were incubated for each powder and time period. After immersion, the upper part of the test solution was decanted into a 15 mL centrifuging tube and the particles were separated from the solution by centrifugation at 3000 rpm (704g) for 10 min. Any floating particles on the solution surface were carefully removed by Pasteur pipettes before pouring the supernatant particle-free solution from the centrifuging tubes into a storage vessel. This separation technique has previously been shown successful and verified using light scattering techniques for similar particles (Hedberg et al., 2010a). A successful particle separation was also evident from the small variation in concentration between replicate samples. Finally, approximately 20 and 140 μL of 65% ultrapure $HNO_3$ were added to the samples to decrease the pH to below 2 and to conserve the samples, a standard procedure for metal analysis.

All vessels and tools were acid-cleaned in 10% $HNO_3$ for at least 24 h, rinsed four times in ultrapure water (18 MΩ cm), and dried in ambient laboratory air. All chemicals used were of analytical grade (p.a.), or puriss p.a. grade (in the case of nitric acid used for acidification of the samples).

**Table 2**
Chemical composition (g/L) of artificial biological fluids.

| Chemicals | ALF pH 4.5 | ASW pH 6.5 |
|---|---|---|
| $MgCl_2$ | 0.0497 | – |
| NaCl | 3.210 | 5.000 |
| $Na_2HPO_4$ | 0.071 | – |
| $Na_2SO_4$ | 0.039 | – |
| $CaCl_2.2H_2O$ | 0.128 | – |
| NaOH | 6.000 | – |
| Citric acid | 20.80 | – |
| Glycine | 0.059 | – |
| $C_6H_5Na_3O_7{\cdot}2H_2O$ | 0.077 | – |
| $C_4H_4O_6Na_2{\cdot}2H_2O$ | 0.090 | – |
| $C_3H_5NaO_3$ | 0.085 | – |
| $C_3H_3O_3Na$ | 0.086 | – |
| $(NH_2)_2CO$ (urea) | – | 1.000 |
| $CH_3CHOHCO_2H$ (lactic acid) | – | 1.000 |

Artificial lysosomal fluid (ALF), pH 4.5, artificial sweat (ASW), pH 6.5.

### 2.4. Solution analysis

Total nickel concentrations in the solution samples were analyzed by means of flame atomic absorption spectroscopy, Flame-AAS (Perkin Elmer AAnalyst 800). The solution samples were diluted with ultrapure water when necessary to increase the solution volume. All analyses were based on three replicate readings for each solution sample, and a quality control sample of known concentration was also analyzed. Calibration was conducted with ultrapure water and four metal standards of 2, 6, 20, and 60 mg/L Ni. All presented results are based on the mean values and standard deviation of the triplicate samples for each material, solution, and time period (nine measurements) with the respective blank sample concentration, if any, subtracted. Typical blank concentrations were <0.091 mg/L. The limits of detection (LOD) were 0.015 and 0.023 mg/L for ALF and ASW solution samples, respectively.

### 2.5. Calculations

Both the released percentage (nickel measured in solution after exposure divided by the amount of nickel powder exposed,

multiplied by 100) and the nickel release rate ($\mu g/cm^2/h$) are presented. As the nickel release rate is normalized on the surface area, the surface area was adjusted considering the (partially large) amount of nickel that was dissolved. Hence, the nickel release rate was efined as below:

$$\text{Ni release rate}[\mu g/cm^2/h] = (c[\mu g/L] * V[L])/(A[cm^2] * t[h]) \quad (1)$$

In which $c$ is the nickel concentration (measured via AAS), $V$ is the solution volume, $A$ is the surface area of the test item ($A$ = (particle mass [g]) * (BET surface area [$m^2/g$])), and $t$ is the exposure time.

Since the dissolution of particles with time causes a reduction of the surface area, the metal release rate was calculated based on a changed surface area over time. To recalculate the surface area, all particles were assumed spherical and of the same size and all particles to dissolve with the same rate. Based on these assumptions, the surface area can be calculated as $(\sqrt[3]{(x\%/100)})^2$ times the original surface area of spherical particles (from BET measurements), where $x\%$ is the dissolved percentage after a given time period.

## 3. Results and discussion

### 3.1. Powder morphology and size

Differences in morphology of the nickel and nickel oxide powders are elucidated via field emission gun scanning electron microscopy (FEG-SEM) images in Fig. 1. Both nickel metal powders contained spherical particles, whereas individual particles of nickel oxide were significantly larger in size and had a broader size distribution. These observations are in agreement with measured BET areas (Table 1) that are significantly smaller for NiO (N46) compared to the nickel metal powders; NiO (N46, 0.25 $m^2/g$) < Ni (N13, 1.05 $m^2/g$) < Ni (N36, 2.15 $m^2/g$).

Differences in particle size distributions are presented in Fig. 2 (a: mass, b: numbers) and compiled in Table 3, for the different powders in ASW, as determined by means of LALLS.

According to Fig. 2a (mass) and b (number), the average particle size in solution increased according to the following sequence: Ni (N36) < Ni (N13) < NiO (N46). Larger agglomerates (average size at approximately 100 μm) were evident for both nickel metal powders, especially pronounced in the case of Ni (N36), Fig. 2a. The NiO (N46) powder revealed the presence of very fine particles sized between 0.2 and 1 μm in diameter, c.f. Figs. 1 and 2. Particle sizing in the PBS medium indicated a very similar distribution behavior (data not shown).

### 3.2. Bulk and surface composition

Despite the use of a laser intensity and accumulation time as low as possible to obtain any spectra, it was not possible to generate any reliable confocal Raman spectroscopy spectra for the nickel metal powders. The signal was either too weak or the samples became oxidized by the laser beam, observed as black spots after visual examination after each measurement. Reliable spectra were however possible to generate for the bulk NiO (N46) powder with peak positions in agreement with literature findings (Cordoba-Torresi et al., 1991; Dharmaraj et al., 2006; Dietz et al., 1971). Two strong broad peaks were observed at 550 and 1083 1/cm (very strong) and weaker broad peaks at 164, 240, 350 (very weak), 740, and 900 1/cm (very weak). No peaks assigned to hydroxides or other nickel oxides were identified by Raman spectroscopy, possibly a consequence of its low surface sensitivity in the case of bulk NiO powder. This may be explained by the fact that most nickel oxides and hydroxides are poor Raman scatterers (Cordoba-Torresi et al., 1991) and reported peaks mainly derived from lattice imperfections (Dietz et al., 1971).

The oxidation state of nickel in the outermost (5–10 nm) surface oxide of all powders was therefore analysed by means of X-ray Photoelectron Spectroscopy (XPS) generating high-resolution spectra of Ni 2p and O1s, Fig. 3. Consistent with literature findings for NiO, the green NiO (N46) powder revealed a distinct Ni $2p_{3/2}$ photoelectron peak at 854.0 eV in addition to multiplet-split main peaks at 856.0 and 861.0 eV, and a characteristic sharp oxygen peak (O 1s) at 529.7 eV (Casella et al., 1999; Kim and Winograd, 1974). The presence of an additional peak at 531.8 eV (O 1s) could be assigned to small amounts of $Ni(OH)_2$ as the corresponding nickel peak at 855.8 eV may be hidden behind the split peaks of NiO and since negligible oxidized carbon was detected on the surface. The atomic Ni/O ratio was close to 1, which suggests NiO to be the dominating compound with possibly minor amounts of $Ni(OH)_2$ (Casella et al., 1999; Kim and Winograd, 1974). XRD confirmed the presence of crystalline NiO.

The nickel metal powder (Ni (N36)) revealed a similar outermost surface composition compared with the NiO (N46) powder judged from the Ni $2p_{3/2}$ peak at 853.8 eV (XPS), the multiplet split peaks and the O 1s peak at 529.7 eV (Casella et al., 1999; Kim and Winograd, 1974). A higher relative intensity of the main multiplet peaks

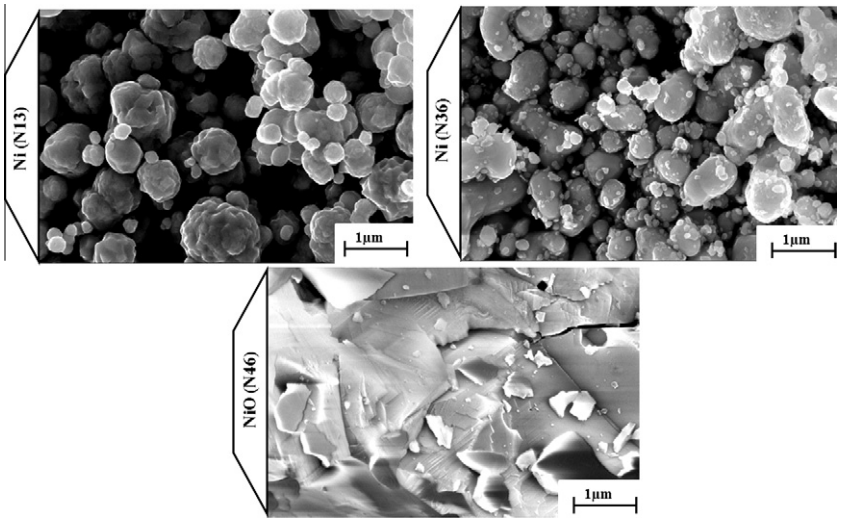


**Fig. 1.** FEG-SEM images (magnification 5000×) of two different nickel metal powders (Ni (N13), Ni (N36)) and a green nickel oxide (NiO (N46)) powder.

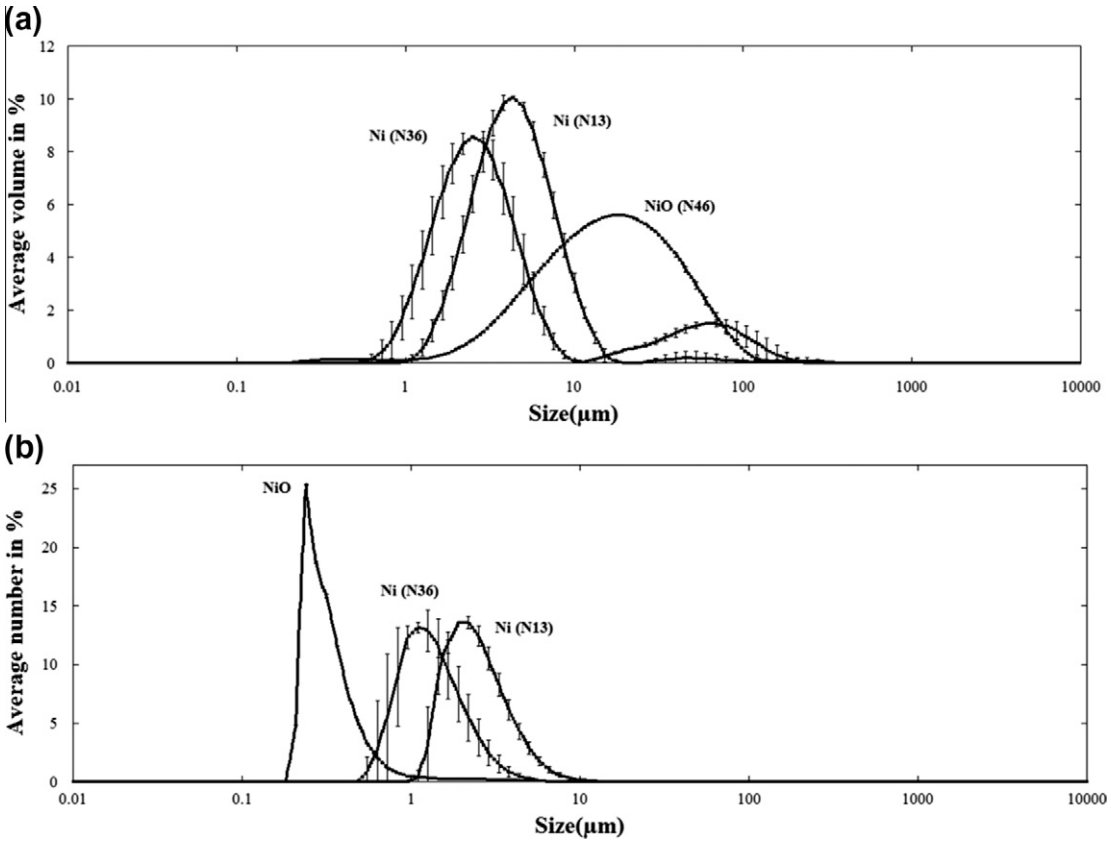


**Fig. 2.** Particle size distributions of NiO (N46) and the Ni metal powders by means of LALLS expressed as; (a) average volume (mass), and (b) average number of Ni (N13), Ni (N36), and NiO (N46) powders. Data represent average values of six replicate measurements.

**Table 3**
Particle size distribution for NiO (N46) and the Ni-metal (N13 and N36) powders in artificial sweat (ASW, pH 6.5) by means of laser diffraction, LALLS. $d_{0.5}$ is the median particle diameter and $d_{0.1}$ and $d_{0.9}$ the 10% and 90% size distribution cut off points, respectively, presented as volume (mass) and numbers.

| | Unit | NiO (N46) | Ni (N13) | Ni (N36) |
|---|---|---|---|---|
| Volume/diameter (µm) | $d_{0.1}$ | 4.7 ± 0.01 | 2.4 ± 0.2 | 1.5 ± 0.2 |
| | $d_{0.5}$ | 17.1 ± 0.09 | 4.6 ± 0.3 | 3.1 ± 0.4 |
| | $d_{0.9}$ | 52.8 ± 0.3 | 9.3 ± 0.9 | 52.9 ± 13.5 |
| Number /diameter (µm) | $d_{0.1}$ | 0.2 | 1.6 ± 0.1 | 0.9 ± 0.2 |
| | $d_{0.5}$ | 0.3 | 2.5 ± 0.2 | 1.3 ± 0.2 |
| | $d_{0.9}$ | 0.6 ± 0.002 | 4.5 ± 0.3 | 2.4 ± 0.3 |

(855.8 and 860.9 eV) compared to the main nickel peak, not observed for NiO (N46), and the presence of an O 1s peak at 531.2 eV suggest the presence of an additional nickel compound, possibly $Ni_2O_3$ (Ni 2p3/2 – 855.8 eV; O1s – 531.7 eV) known as a defect structure of NiO induced by excess oxygen (Casella et al., 1999; Kim and Winograd, 1974; McIntyre and Cook, 1975). The presence of amorphous $Ni(OH)_2$ can however not be excluded (Kim and Winograd, 1974) as no crystalline peaks were observed with XRD. Using a calculated relative area distribution of 1:0.60 between the main peak and the multiplet peaks observed for the green NiO (N46) powder, an approximate relative surface concentration between NiO and $Ni_2O_3$ of 1:2 is suggested. These findings are in line with the literature that claim that NiO is the dominating constituent of the passive film on nickel metal covered with an outer hydroxylated layer, or with a defect-rich surface oxide such as non-stoichiometric NiO or $Ni_2O_3$ (MacDougall and Graham, 1995). The presence of crystalline NiO was furthermore confirmed with XRD showing its main diffraction peaks at 2.41, 2.09, 1.48, 1.26 and 1.21 Å (d-values), similar to findings for the NiO (N46) powder.

One Ni metal powder (Ni (N13)) revealed a peak at 852.9 eV (XPS) assigned to metallic nickel (Casella et al., 1999; Kim and Winograd, 1974), not observed for the other nickel metal powder. Its presence suggests a thinner surface oxide compared to that for the Ni (N36) powder. Peaks that were attributable to NiO were either very weak or absent for this powder, in concordance with XRD findings (no crystalline NiO or a too thin surface oxide). Instead, binding energy peaks identified by XPS occurred at 856.1 and 861.4 eV (Ni $2p_{3/2}$) and at 531.6 eV (O 1s), which suggest the dominance of non-stoichiometric NiO or $Ni_2O_3$ (or possibly $Ni(OH)_2$) as only minor satellite peaks occur for metallic nickel. Only metallic nickel peaks were observed with XRD. Amorphous phases cannot be excluded.

### 3.3. Bioaccessibility

To assess the bioaccessibility of nickel from nickel metal and nickel oxide powders, kinetic studies of nickel release into artificial lysosomal fluid (ALF, pH 4.5, 37 °C), of relevance for inhalation toxicity and/or carcinogenicity, and artificial sweat (ASW, pH 6.5, 30 °C), relevant for skin sensitization and of less acidity compared to ALF, were conducted for up to 24 h. The released percentage of the nickel content of the different powders and corresponding release rates based on recalculated surface area, c.f. experimental section (normalized to the immersion periods (0.5, 2, 6, and 24 h) and the corrected particle BET-surface area) are presented in Figs. 4 and 5, respectively.

Exposure to both ALF and ASW resulted in very low released amounts of nickel from the NiO (N46) powder, less than 0.1% and 0.02%, respectively. Corresponding amounts of nickel released from the nickel metal powders were significantly higher in both fluids.

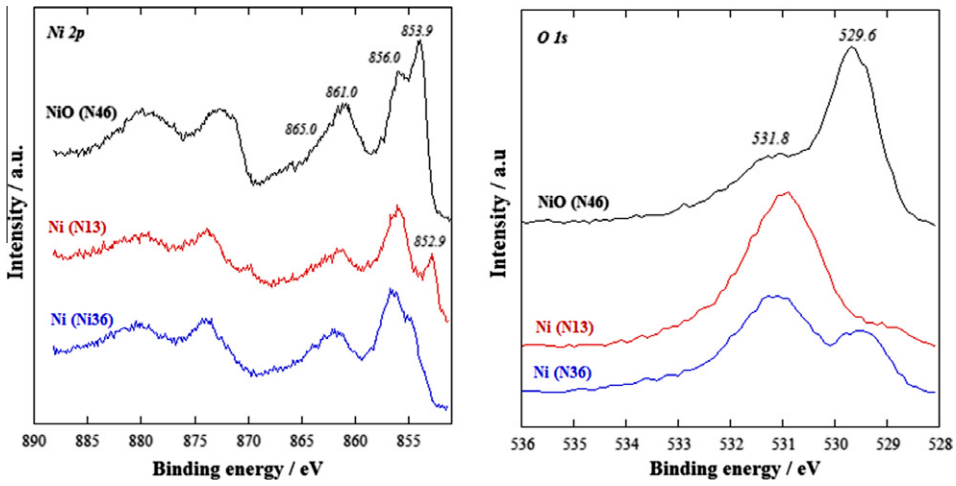


**Fig. 3.** High resolution Ni 2p (left) and O 1s (right) XPS spectra of green NiO (N46) (top) and nickel metal powders (Ni (N13)-middle, Ni (N36)-bottom). Spectra are off-set for clarity.

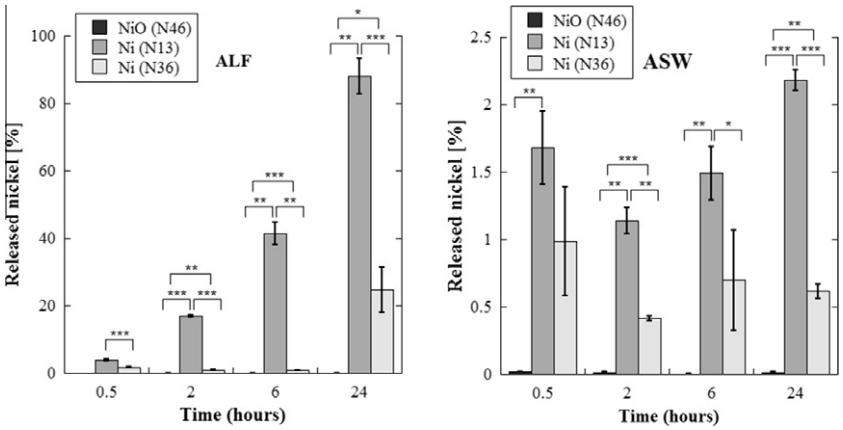


**Fig. 4.** Released amount of nickel from the total nickel content of the exposed powder (dissolved percentage) [%] from nickel metal powders (Ni (N13) and Ni (N36)) and a NiO (N46) powder into ALF (artificial lysosomal fluid, pH 4.5, 37 °C) and ASW (artificial sweat, pH 6.5, 30 °C), respectively. Results represent the mean value and standard deviation between three replicate samples, with the respective blank sample concentration subtracted. The asterisks indicate significant differences: *($p < 0.05$), **($p < 0.01$), and ***($p < 0.001$), as calculated by a student *t*-test (unpaired data with unequal variance).

Exposure in ALF, the more acidic fluid, resulted in an increased released amount of nickel for the nickel metal powders. After 2 h, 17% of the total powder mass of the Ni (N13) powder was dissolved and almost completely dissolved, 88%, after 24 h of exposure. For the Ni (N36) powder, corresponding numbers were significantly lower, ≈1 and 25%. The trend with higher released amounts of nickel from the Ni (N13) nickel metal powder compared to the Ni (N36) powder remained also in ASW of near-neutral pH, although at significantly lower levels (Ni (N13): less than 2.2% and Ni (N36): less than 1%). In ASW, most nickel was released during the first 0.5 h of exposure for both powders followed by minor released amounts during the subsequent exposure period for Ni (N36) and only slightly increased amounts for Ni (N13) during the time period between 4 and 24 h. These results are in concordance with previous findings for nickel powder exposed in artificial sweat (ASW) (Midander et al., 2007). The released amounts of nickel normalized to the corrected surface area correspond to very low rates in ASW after 24 h, lower than 0.003 μg/cm$^2$/h for NiO (N46), and lower than 0.1 and 0.01 μg/cm$^2$/h for Ni (N13) and Ni (N36), respectively (<0.03, <1, and <0.4 μg/cm$^2$/h, after 0.5 h, respectively). Corresponding rates in ALF (24 h) were less than 0.01, 21 and 0.7 μg/cm$^2$/h for NiO (N46), Ni (N13) and Ni (N36), respectively. It is evident that other characteristics than differences in surface area account for differences in release rates both for powders of the same substance (nickel metal) or across substances (nickel oxide and nickel metals).

In all, the results clearly show that the release of nickel was significantly higher from the nickel metal powders compared with the nickel oxide powder in both ALF and ASW: Ni (N13) > Ni (N36) ≫ NiO (N46), Figs. 4 and 5. The release of nickel from the nickel oxide was 65–2100 times lower compared with the nickel metal powders in ALF, effects evident, though less pronounced in ASW (1–10 times lower). Observed results are in good agreement with literature findings, showing a very low solubility of green NiO samples in biological fluids (Oller et al., 2009; Takahashi et al., 1999). Generated results are consistent with previous investigations of the nickel metal sample N36 (Oller et al., 2009) and lower compared with a different sample of nickel powder of smaller particle size (Kuehn and Sunderman, 1982).

Despite the fact that Ni (N36) had the smallest mean particle size in solution, Table 1 and Fig. 2, and the largest BET surface area among the examined powders, significantly more nickel was released from the Ni (N13) powder, both when expressed as percentage of released nickel and release rate. This indicates that the

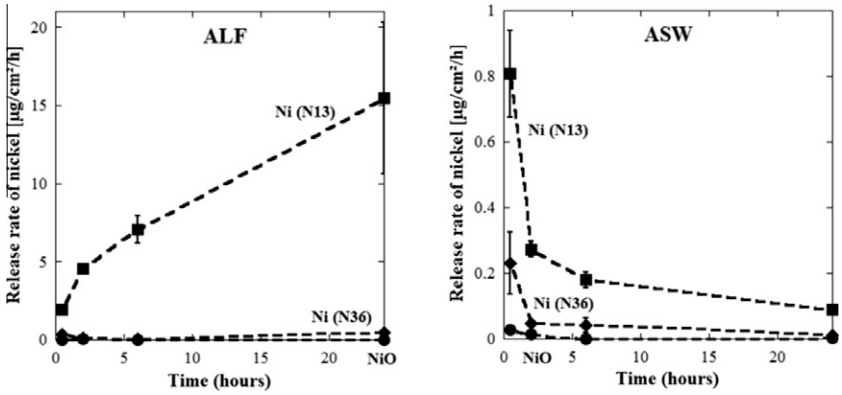


**Fig. 5.** Nickel release rates based on recalculated surface areas after each time period, c.f. experimental section, for nickel metal powders (Ni (N13) and Ni (N36)) and a NiO (N46) powder exposed for 0.5, 2, 6, and 24 h in ALF (artificial lysosomal fluid, pH 4.5, 37 °C), left, and ASW (artificial sweat, pH 6.5, 30 °C), right.

specific surface area and particle size cannot solely explain observed differences in nickel release from the nickel metal powders.

Comparing the results for the two nickel metal powders, exposure in ALF resulted in a significantly higher extent and a different time dependence of released nickel from the Ni (N13) powder compared with the Ni (N36) powder. These results are believed to be correlated to differences in the outermost surface composition as depicted with XPS, c.f. discussion above. The Ni (N13) powder revealed a thinner surface oxide, the lack, or minor presence, of NiO, and the possible presence of a defect-rich surface oxide of $Ni_2O_3$ (or $Ni(OH)_2$) of presumably lower passive properties, compared with the Ni (N36) powder with a thicker surface oxide of NiO covered with $Ni(OH)_2$ and/or $Ni_2O_3$.

In ASW, most nickel was released during the first 0.5 h of exposure for both nickel powders, which is reflected in strongly decreasing nickel release rates with time (Fig. 5). This time dependence is also known for other passivating materials, such as stainless steel, in non-complexing solutions and solutions of near-neutral pH (Hedberg et al., 2010b; Midander et al., 2010). As previously discussed, the release of nickel was significantly higher in ALF compared with ASW for all powders, Figs. 4 and 5, an effect believed to be mostly related to the presence of complexing agents such as citric acid in ALF, in addition to the lower pH (Hedberg et al., 2011). In contrast to ASW, the release rate was increasing for the nickel particles, when considering their real surface area, indicative of non-passive conditions. Kinetic differences in ALF and ASW for the nickel metal powders may be related to the relatively slow (and postponed) complexation process of citrate with nickel in ALF, the predominating release mechanism in the case of stainless steel powders (Hedberg et al., 2011). This process is expected to be of even more importance to nickel powders, compared with stainless steel, since nickel(II)–citrate complexes have higher stability constants compared with other metals such as iron(II) or chromium(III) (Stumm and Morgan, 1996). However, stability constants cannot alone predict the extent of complexing-agent-induced metal release, which further requires information on stability and composition of the surface oxide, previously elucidated for stainless steel powders (Hedberg et al., 2011). The importance of the surface oxide characteristics is evident also in this study where nickel monoxide seems to be the most stable protecting oxide compared with other nickel oxides/hydroxides formed. The thickness of the surface oxide is probably another factor of importance for its barrier effects and dissolution properties. In the case of Ni (N36) particles immersed into ALF media, the low amount of released nickel over the first 6 h (with an average amount of released mass of 1.2%) followed by a significant increase nickel released after 24 h of exposure (about 25%) could also be explained by stable oxide defects induced by complexation with citrate. This "breakdown" was previously not observed for massive nickel metal sheet up to 1 week of exposure (Herting et al., 2008).

Results of this study are somehow contradictory to a reported study where the dissolution of an ultrafine sample of NiO powder was largest in deionized water compared with solutions containing salt or proteins (Yamada et al., 1993). However, reported findings in many other studies (Horie et al., 2009; Julien et al., 2011; Kodama et al., 1985, 1993; Kuehn and Sunderman, 1982; Oller et al., 2009; Sunderman et al., 1987; Tanaka et al., 1986) are in line with observations in this study with remarkably lower released amounts of nickel from NiO in deionized water compared with more complexing solutions containing chlorides, citrate, amino acids or proteins.

Large variations in the metal release behavior between different types of NiO powders seem mainly to be related to differences in physico-chemical properties (size, chemical composition, surface area, crystallinity, temperature of calcining, content of Ni(III)) (Horie et al., 2009; Kodama et al., 1993; Sunderman et al., 1987; Takahashi et al., 1999; Yamada et al., 1993). For example, Ni(III) containing oxides (e.g., $Ni_2O_3$) were found to be more potentially toxic compared to Ni(II) containing oxides (e.g., NiO) and believed to be more soluble and hence less corrosion protective compared to NiO (Sunderman et al., 1987; O'Brien and Salacinski, 1996). These observations are in agreement with observations of this study suggesting the lack or minor presence of NiO and the presence of a defect-rich $Ni_2O_3$ surface oxide (or possibly $Ni(OH)_2$) on the Ni (N13) powder with higher nickel release compared to the Ni (N36) powder with predominant NiO present on the surface. In a previous study (Sunderman et al., 1987), it was suggested that the presence of Ni(III)-species and/or nickel hydroxides in a NiO powder was the reason for its higher induced biological effects such as cytotoxicity compared with other NiO powders of the same color and dissolution half times (based on nickel release rates up to 72 h) in water and body fluids.

Most probably, the initial surface conditions present on the samples before the study began, as investigated here, are responsible for the observed differences between the nickel metal powders. In ALF, a "breakdown" of the barrier properties of the surface oxide was observed for both nickel metal powders, but after different time periods. After this breakdown, the corrosion process is expected to induce significant changes in the oxide/corrosion products on the particle surface as well as on the particle size. This was not fully investigated due to the low particle mass exposed to the synthetic fluids in this study and still remaining after exposure. The corrosion products are however expected to be of similar composition for both nickel metal samples and the change in particle size with time was taken into account by the theoretical recalculations of the surface area (Fig. 5).

### 3.4. Comparison with literature findings for nickel metal and nickel oxide, powder and massive forms

An overview on literature findings on nickel release data from nickel metal and nickel oxide powders, and massive nickel metal is presented in Table 4 and compared with data generated in the present study. Since the specific surface area (BET area) was not always reported, the dissolved percentage of the total nickel content of the investigated materials is preferentially given. For massive materials, the metal release rate is given.

#### 3.4.1. Effect of solution

Consistent with findings of this study, the literature survey showed a clear trend for increased release of nickel both from nickel metal and nickel oxide powders with decreasing solution pH and increasing solution complexation capacity, Table 4.

#### 3.4.2. Effect of particle size and agglomeration

The release of nickel from nickel metal powders varies among and within reported studies and was shown to be highly dependent on particle characteristics such as particle size, agglomeration and surface composition. The extent of nickel release from nickel metal powders was reported to decrease with higher particle loading (surface area/particle mass to solution volume ratio) due to agglomeration and possibly equilibrium shifts (Hamel et al., 1998; Midander et al., 2006, 2007; Turner, 2011). The nickel metal sample (N36) has been tested at two significantly different loadings, 2 g/L (Oller et al., 2009) and 0.1 g/L (this work). However, since the testing solutions were not identical, the true effect of loading on the nickel release from this sample cannot be assessed. The effect of particle size was most obvious when comparing a study on NiO nanoparticles (BET area 75 $m^2$/g, (Pietruska et al., 2011)) in cell culture medium with other studies on fine micron-sized particles in other media (this study, (Oller et al., 2009)). Even though the surface area of the NiO nanoparticles was approximately 300 times larger compared with the powder of this study and the study of Oller et al. (2009), the nanoparticles dissolved to a significantly higher extent (a factor of 100–5000 or more). However, as nanoparticles possess significantly different properties compared to micron-sized particles (Nyborg et al., 1992), e.g. surface atoms to bulk atoms ratio, they shall not directly be compared to results of micron-sized particles.

#### 3.4.3. Ni metal powders

The release of nickel from the two nickel metal powders of this study is in close agreement with literature findings. An example is when compared with larger sized nickel metal powders (BET area 0.43 $m^2$/g) exposed in ASW (Midander et al., 2007) and ALF (Hedberg et al., 2010a), Table 4, which shows a higher release compared with N36, but a lower release compared with N13, when accounting for the surface areas. This clearly elucidates the importance that other parameters in addition to the surface area govern the release process.

#### 3.4.4. NiO powders

Approximately 10 times less nickel was released from the NiO (N46) powder of this study compared with results reported elsewhere. Oller et al. (2009) exposed another NiO sample (N9) to solutions of similar pH and complexing capacities as ALF (e.g., 0.1 M ammonium citrate, 0.1 M citric acid, Table 4). Observed differences are in this case most probably due to smaller sized NiO particles (2.6 $m^2$/g) in the study of Oller et al. (2009) compared with this study (0.25 $m^2$/g). In a recent study, a sample of green NiO powders of different particle size was studied in intestinal fluid (pH 7.4), showing a dissolution of 0.01% (BET area 0.01 $m^2$/g) and 0.12% (BET area 2.62 $m^2$/g) after 24 h of exposure (Henderson et al., 2012), comparable to the NiO (N46, BET 0.25 $m^2$/g) powder here in artificial sweat (pH 6.5) with 0.01% dissolution after 24 h. Sunderman et al. (1987) reported higher dissolution of jet black NiO powder (dissolution half time: 0.8 year) compared to grey or green NiO powder (dissolution half time longer than 11 years) exposed in rat serum, and even less dissolution in renal cytosol and water.

#### 3.4.5. Comparison between NiO and Ni powders

When comparing similar particle sizes, the release from nickel oxide powders was generally significantly lower compared with nickel metal powders, an effect observed in this study and also evident from the study of Oller et al. (2009).

#### 3.4.6. Comparison to massive nickel metal samples

When comparing the release of nickel from nickel metal powders in ALF (this study) with release of nickel from massive abraded nickel metal sheet exposed in ALF (Herting et al., 2008), more nickel was released from massive sheet compared to the powder at similar exposure conditions, 16.8 μg/$cm^2$/h compared with 0.5–15.5 μg/$cm^2$/h, Table 4. This is most probably an effect of freshly abraded surfaces of the massive metal sheets, whereas the powder was exposed in its as-received condition with aged surface oxides. However, the time dependence was different for massive sheet, with decreasing nickel release rates over time, while the nickel powders investigated in this study revealed increasing rates over time and/or showed a significant increase after 6 h of exposure (N 36). This indicates that powder particles that are dissolved, and hence reduced in size, can become more active with time.

### 3.5. Comparison to literature findings for nickel-containing alloys

When comparing the release of nickel from nickel-containing alloys, Table 5, to the release from pure nickel metal, it was evident that both surface properties and galvanic corrosion properties (in the case of Cu75Ni25) play a more important role for the nickel release than the bulk content. All studies on nickel-containing (9–10 wt.%) stainless steel, both as powders and massive sheet, indicate that stainless steel releases very low amounts of nickel, despite its relatively high nickel metal content. For example, reported release rates of nickel from powders and massive sheet of stainless steel exposed in ALF are in the range of 0.003–0.005 μg Ni/$cm^2$/h, after 24 h (Table 5), which corresponds to 0.03–0.05 μg Ni/$cm^2$/h when normalizing to their bulk alloy nickel content. Corresponding release rates of nickel from the nickel metal powders of this study are 0.4–3.5 μg/$cm^2$/h (Table 4). In contrast, from the Cu75Ni25 alloy, used in coins, more nickel (factor 10–50) was released into ASW when compared both to massive nickel metal (also used in coins) (Lidén and Carter, 2001), and to nickel metal powders (this study), Tables 4 and 5. This is most probably due to galvanic effects, since de-alloying of less noble alloying elements (nickel in this case) is a known phenomenon for copper alloys (Marshakov, 2002).

### 3.6. Implications for nickel-induced toxicity

While skin irritation induced by nickel metal and nickel oxide particles seem to be solely related to released soluble nickel species, i.e. the *bioaccessible fraction* (Flint, 1998; Lidén and Carter, 2001; Lidén et al., 2008; Midander et al., 2007), the respiratory toxicity of nickel metal and inorganic nickel compounds is assumed to be related to the bioavailability of two-valent nickel ions at target extracellular or intracellular sites (Goodman et al., 2011). For local effects, these sites can be the respiratory cells after inhalation (extra and/or intracellular levels) or the dermal cells after skin exposure. For systemic effects (e.g., kidney effects), the target sites

**Table 4**
Dissolved percentage of total nickel content or – where not available – release rate of nickel from nickel and green nickel oxide powders, in dependence of exposure time periods and solutions. Note the difference in surface area and particle sizes (refer to footnotes)!.

| | DI water (pH 6.3) | Ammonium citrate (pH 4.4) | Citric acid (pH 2.1) | Interstitial fluid (pH 7.4) | Alveolar fluid (pH 7.4) | Cell culture medium | DMDM + 10% FBS | Fresh water medium (pH 6.0) | Artificial sweat, ASW (pH 6.5) | Artificial lysosomal fluid, ALF (pH 4.5) |
|---|---|---|---|---|---|---|---|---|---|---|
| *Ni metal powders, dissolved percentage of nickel content* | | | | | | | | | | |
| 0.5 h | | | | | | | | | 1.7%[b]; 1.0%[c] | 4%[b]; 1.8%[c] |
| 1 h | 0.18%[a] | 0.52%[a] | 0.81%[a] | 0.14%[a] | 0.16%[a] | | | | | |
| 2 h | | | | | | | | | 1.1%[b]; 0.4%[c] | 17%[b] (4.9 μg/cm$^2$/h); 0.9%[c] (0.045 μg/cm$^2$/h) |
| 6 h | | | | | | | | | 1.5%[b]; 0.7%[c] | 41%[b]; 0.9%[c] |
| 12 h | | | | | | | | | 0.21%[d] | |
| 24 h | 0.18%[a] | 4.01%[a] | 43.8%[a] | 0.16%[a] | 0.23%[a] | ≈0.4%[e] | | 0.3%[f] | 2.2%[b] (0.09 μg/cm$^2$/h); 0.6%[c] (0.01 μg/cm$^2$/h) | 88%[b] (15.5 μg/cm$^2$/h); 24%[c] (0.7 μg/cm$^2$/h) |
| 1 week | | | | | | | | | | 87%[g] |
| *NiO powders, dissolved percentage of nickel content* | | | | | | | | | | |
| 0.5 h | | | | | | | | | 0.02%[h] | <LOD[h] |
| 1 h | | | | | | | | | | |
| 2 h | | | | | | ≈38%[i] | | | 0.02%[h] | 0.09%[h] |
| 6 h | | | | | | | | | 0.003%[h] | 0.03%[h] (0.01 μg/cm$^2$/h) |
| 12 h | | | | | | ≈45%[i] | | | | |
| 24 h | 0.1%[j]; 0.03%[k]; 0.31%[l] | 0.55%[j] | 0.63%[j] | 0.07%[j] | 0.05%[j] | ≈50%[i] | ≈0.05%[k]; ≈5.4%[l] | | 0.01%[h] (0.0017 μg/cm$^2$/h) | 0.04%[h] (0.005 μg/cm$^2$/h) |
| *Ni metal (massive forms)* | | | | | | | | | | |
| 24 h | | | | | | | | | | 16.8 μg/cm$^2$/h[m] |
| 1 week | | | | | | | | | 0.01–0.04 μg/cm$^2$/h[n] | |

*Abbreviations:* LOD – limit of detection; DMDM – DMEM, Dulbecco's modified Eagle's medium; FBS – fetal bovine serum; SEM – scanning electron microscopy; BET – Brunauer Emmet Teller method (specific surface area); ASW – artificial sweat; ALF – artificial lysosomal fluid; DI – deionized.

[a] Particle mean diameter: 1.26 μm (based on SEM), N36 (the same as in this study), BET 2.15 m$^2$/g, loading 2 g/L; 37 °C, (Oller et al., 2009).
[b] this study, Ni powder N13; median diameter: 2.4 μm (based on number%)–4.9 μm (based on volume%), BET 1.05 m$^2$/g, loading 0.1 g/L, 37 °C in ALF, 30 °C in ASW.
[c] This study, Ni powder N36; median diameter: 1.5 μm (based on number%)–3.1 μm (based on volume%), BET 2.15 m$^2$/g, loading 0.1 g/L, 37 °C in ALF and 30 °C in ASW.
[d] BET 0.43 m$^2$/g, loading 0.2 g/L, 30 °C, (Midander et al., 2007).
[e] <100 nm Ni: 4.4 m$^2$/g, loading 5 μg/cm$^2$, 37 °C, (Pietruska et al., 2011).
[f] BET 0.43 m$^2$/g, 20 °C, loading 0.1 g/L, (Skeaff et al., 2011).
[g] BET 0.43 m$^2$/g, loading 0.2 g/L, 37 °C, (Hedberg et al., 2010a).
[h] this study, NiO (N46) powder, median diameter 0.3 μm (based on number%)–17.3 μm (based on volume%), BET: 0.25 m$^2$/g, loading 0.1 g/L, 37 °C in ALF and 30 °C in ASW.
[i] <100 nm NiO powder: 75 m$^2$/g, loading 5 μg/cm$^2$, 37 °C, (Pietruska et al., 2011).
[j] Particle mean diameter: 3.5 μm (based on SEM); ID: N9, 2.62 m$^2$/g, loading 2 g/L; 37 °C, (Oller et al., 2009).
[k] BET 3.44 m$^2$/g, loading 10 g/L, 37 °C, (Horie et al., 2009).
[l] BET > 6 m$^2$/g, loading 10 g/L, 37 °C, (Horie et al., 2009).
[m] Abraded Ni metal, 37 °C, (Herting et al., 2008).
[n] 30° (Lidén and Carter, 2001).

**Table 5**
Dissolved percentage of total nickel content or – where not available – release rate of nickel from stainless steel powders, a massive Cu75Ni25 alloy, and massive stainless steel grades, in dependence of exposure time periods and solutions. Note the difference in surface area and particle sizes (refer to footnotes)!.

| | Artificial sweat, ASW (pH 6.5) | Artificial lysosomal fluid, ALF (pH 4.5) |
|---|---|---|
| *Stainless steel powders (316L)* | | |
| 24 h | <0.0004 μg/cm$^2$/h[a] | 0.005 μg/cm$^2$/h[b] |
| 1 week | <0.00006 μg/cm$^2$/h[a] | 0.9%[c] |
| *Cu75Ni25 (coins)* | | |
| 24 h | 1.5–2.5 μg/cm$^2$/h[d] | |
| 1 week | 0.19–0.27 μg/cm$^2$/h[e]; 0.5–0.8 μg/cm$^2$/h[d] | |
| *Stainless steel (massive forms)* | | |
| 8 h | | 0.001–0.002 μg/cm$^2$/h[f]; 0.009 μg/cm$^2$/h[g] |
| 24 h | | 0.003 μg/cm$^2$/h[g] |

*Abbreviations:* BET – Brunauer Emmet Teller method (specific surface area); ASW – artificial sweat; ALF – artificial lysosomal fluid.
[a] AISI 316L powder <4 μm, Ni content 10 wt.%, BET 0.7 m$^2$/g, loading 0.1 g/L, 30 °C, (Hedberg et al., 2010b).
[b] AISI 316L powder <4 μm, Ni content 10 wt.%, BET 0.7 m$^2$/g, loading 0.1 g/L, 37 °C, (Hedberg et al., 2011).
[c] AISI 316L powder <4 μm, BET 0.7 m$^2$/g, loading 0.1 g/L, 37 °C, (Hedberg et al., 2010a).
[d] 30 °C, (Lidén et al., 2008).
[e] 30 °C, (Lidén and Carter, 2001).
[f] AISI 304, Ni content 9 wt.%, 37 °C, (Herting et al., 2006).
[g] AISI 316L, as-received, Ni content 10 wt.%, 37 °C.

may be particular cells within that organ. Bioaccessibility of released nickel in synthetic biological fluids can be used as a surrogate to estimate bioavailability. The bioaccessibility results from this study provide therefore information regarding biological effects of nickel metal and oxides.

Both extra and intracellular dissolution may contribute to respiratory toxicity of Ni-containing particles after inhalation. Based on the relative nickel release results in ALF (as representative of the intracellular cell environment), nickel metal powders are predicted to be more cytotoxic to the respiratory tract compared with nickel oxide powders. These results are consistent with in vivo results from repeated inhalation exposure studies conducted in rats (NTP, 1996; Oller et al., 2008). One of the nickel metal powders (N36) investigated in this study was also (without any modification) tested in a rat inhalation study and revealed a toxicity LOAEC value of 4 mg/m$^3$ in a 28 day study, and a LOAEC value of 1 mg/m$^3$ in a 13 week study (Oller et al., 2008). The same nickel oxide powder (high calcining temperature, green) investigated in this study (N46) resulted in a LOAEC of 30 mg/m$^3$ (NOAEC = 10 mg/m$^3$) in a 16 day study, and a LOAEC of 5 mg/m$^3$ in a 13 week study (NTP, 1996). In the NTP study, the NiO powder (N46) was milled to generate an appropriate size animal aerosol.

For carcinogenicity, however, the nickel release is only one of many factors that determine tumor induction (Goodman et al., 2011; Muñoz and Costa, 2012). A recent review describing the bioavailability model, explains why NiO particles show carcinogenicity in contrast to nickel metal particles (Goodman et al., 2011). A substance must necessarily fulfil a number of factors to cause cancer: (i) the particles must be sparingly soluble (highly soluble particles may be highly toxic, but will not cause cancer, since they are dissolved before they can be endocytosed) (Dunnick et al., 1995; Goodman et al., 2011; Miura et al., 1989; Oller et al., 1997), (ii) the particle size must be smaller than 4–5 μm to be endocytosed (Costa et al., 1981; Muñoz and Costa, 2012; Evans et al., 1982), (iii) the intracellular dissolution of the particles must be sufficient (not too high or low) to allow nickel ions to reach the nucleus without causing cell death (Goodman et al., 2011), and (iv) the in vivo clearance time of the particles must be sufficiently long (Goodman et al., 2009, 2011). The combination of these factors appears sufficient to yield respiratory tumors in the rat inhalation studies with nickel oxide (a milled version of the same NiO sample studied in this study) but not with nickel metal (same sample studied in this study). It is clear then that in the case of nickel, the nickel ion release, by itself, cannot predict carcinogenic outcome.

In a recent review (Muñoz and Costa, 2012), endocytosis mechanisms of nickel-containing powder particles were discussed. The authors suggest that macropinocytosis and/or clathrin mediated endocytosis is the uptake mechanism for insoluble nickel particles and not phagocytosis, as previously thought. The importance of different particle characteristics and surface properties, i.e. particle size, surface charge, bulk and surface structure (crystallinity), was underlined (Abbracchio et al., 1982).

Therefore, the mechanisms for respiratory nickel toxicity and carcinogenicity are different, as evident by the opposite profile displayed by nickel metal powders and oxides: higher toxicity and negative respiratory carcinogenicity for nickel metal and lower toxicity and positive respiratory carcinogenicity for nickel oxide in animal studies. The in vivo results are consistent with observed differences in physico-chemical properties, i.e. particle size distribution and bioaccessibility (released nickel fraction), described and highlighted in this paper.

## 4. Concluding remarks

This investigation clearly shows significant differences in particle characteristics, surface composition and release of nickel from nickel metal powders with thin outer surface oxides (shells) compared with release of nickel from a powder of bulk nickel oxide. This emphasizes that release data from nickel compounds (e.g., NiO) cannot be used to assess the behavior of nickel metal (Ni). Chemical dissolution primarily governs the release process of nickel oxide, whereas also electrochemical dissolution processes (i.e., corrosion) take place for the nickel metal powders. Generated results suggest that the relative Ni release from nickel metal and nickel oxide powders will be the results of the interplay between the thickness and composition of the oxide layer on the nickel metal particles, the particle size, the surface area and the nature of the particles themselves, all influenced by the process of manufacturing of the material (e.g., calcining temperature, etc.).

More nickel was released from the nickel metal powder (N13, 88% after 24 h in ALF) with an outer thin surface oxide predominantly composed of non-stoichiometric nickel oxide, probably $Ni_2O_3$, compared with the nickel metal powder (N36, 25% release after 24 h in ALF) with a thicker surface oxide primarily composed of NiO and to some extent $Ni_2O_3$. The N13 powder also displayed increasing release rates based on the real (recalculated) surface area when exposed in ALF, an effect not observed in ASW and

possibly related to the presence of complexing agents such as citric acid in ALF, in addition to the lower pH of ALF. In the case of Ni (N36) particles immersed into ALF, a significant increase in nickel released was observed after 24 h (21-fold compared with previous exposure time points) that may be explained by stable defects in the passive surface oxide. This effect has not been observed for massive nickel metal sheet in the literature.

Observations in this study show an enhancement of released nickel in solutions of reduced pH and increased concentration of complexing agents such as citric acid in ALF, an effect also observed in the literature in the presence of e g. chlorides, other salts, amino acids and proteins. Large variations in nickel release observed between different powders reported in the literature are highly dependent on size, particle concentration, solution and hence extent of agglomeration. The release of nickel, in particular from alloys, is non-proportional to the bulk alloy composition. Surface oxide characteristics and composition as well as particle characteristics and solution chemistry governs the release process.

Any toxicological assessments or bioaccessibility investigations of metal powders require in-depth knowledge and understanding of particle characteristics in solution and changes in surface reactivity and composition with time. Lack of data precludes any reliable comparisons between literature data and the assessment of potential hazards and risks.

## 5. Conflict of interest

Financial support was received from Cusanuswerk, Germany (Yolanda Hedberg), Swedish Research Council, VR (Sweden), NiPERA, Inc., USA, and Knut and Alice Wallenberg foundation, Sweden (grant for the XPS instrument). The study sponsors were not involved in the study design, collection, analysis and interpretation of data, the writing of the manuscript, or the decision to submit the manuscript for publication.

## Acknowledgments

Dr. Adriana Oller is acknowledged for in-valuable discussions and NiPERA, Inc. for supplying powder materials. The following sources of financial support to the project and/or to individual authors are acknowledged: Cusanuswerk, Germany (Y.H.), Swedish Research Council, VR (Sweden), NiPERA, Inc. USA, and the Knut and Alice Wallenberg foundation, Sweden (grant for the XPS instrument). The authors are members of the Stockholm Particle Group, an operative network between three universities in Stockholm: Royal Institute of Technology, Karolinska Institutet, and Stockholm University, supported by the Swedish Research Councils VR and Formas. Michael Lundberg at Sandvik Heating Technology, Hallstahammar, Sweden is highly appreciated for performing the BET measurements, and Dan Jacobsson at Swerea Kimab, Sweden for running XRD.

## References

Abbracchio, M.P., Heck, J.D., Costa, M., 1982. The phagocytosis and transforming activity of crystalline metal sulfide particles are related to their negative surface charge. Carcinogenesis 3, 175–180.

Barrientos, L., Rodriguez-Llamazares, S., Merchani, J., Jara, P., Yutronic, N., Lavayen, V., 2009. Unveiling the structure of Ni/Ni oxide nanoparticles system. J. Chil. Chem. Soc. 54, 391–393.

Brunauer, S., Emmet, P.H., Teller, E., 1938. Adsorption of gases in multimolecular layers. J. Am. Chem. Soc. 60, 309–319.

Casella, I.G., Guascito, M.R., Sannazzaro, M.G., 1999. Voltammetric and XPS investigations of nickel hydroxide electrochemically dispersed on gold surface electrodes. J. Electroanal. Chem. 462, 202–210.

Cordoba-Torresi, S.I., Goff, A.H.-L., Joiret, S., 1991. Electrochromic behavior of nickel oxide electrodes. J. Electrochem. Soc. 138, 1554–1559.

Costa, M., Abbracchio, M.P., Simmons-Hansen, J., 1981. Factors influencing the phagocytosis, neoplastic transformation, and cytotoxicity of particulate nickel compounds in tissue culture systems. Toxicol. Appl. Pharmacol. 60, 313–323.

de Meringo, A., Morscheidt, C., Thélohan, S., Tiesler, H., 1994. In vitro assessment of biodurability: acellular systems. Environ. Health Perspect. 102, 1–6.

Denkhaus, E., Salnikow, K., 2002. Nickel essentiality, toxicity, and carcinogenicity. Crit. Rev. Oncol. Hematol. 42, 35–56.

Dharmaraj, N., Prabu, P., Nagarajan, S., Kim, C.H., Park, J.H., Kim, H.Y., 2006. Synthesis of nickel oxide nanoparticles using nickel acetate and poly(vinyl acetate) precursor. Mater. Sci. Eng., B 128, 111–114.

Dietz, R.E., Parisot, G.I., Meixner, A.E., 1971. Infrared absorption and Raman scattering by two-magnon processes in NiO. Phys. Rev. B 4, 2302–2310.

Dunnick, J.K., Elwell, M.R., Radovsky, A.E., Benson, J.M., Hahn, F.F., Nikula, K.J., Barr, E.B., Hobbs, C.H., 1995. Comparative carcinogenic effects of nickel subsulfide, nickel oxide, or nickel sulfate hexahydrate chronic exposures in the lung. Cancer Res. 55, 5251–5256.

EC, 2009. Commission Regulation (EC) No. 790/2009 Amending, or the purposes of its adaptation to technical and scientific progress, Regulation (EC) No. 1272/2008 of the European Parliament and of the Council on Classification, Labelling and Packaging of Substances and Mixtures.

EN, 2011. Reference test method for release of nickel from all post assemblies which are inserted into pierced parts of the human body and articles intended to come into direct and prolonged contact with the skin, vol. EN 1811:2011.

Evans, R.M., Davies, P.J.A., Costa, M., 1982. Video time-lapse microscopy of phagocytosis and intracellular fate of crystalline nickel sulfide particles in cultured mammalian cells. Cancer Res. 42, 2729–2735.

Flint, G.N., 1998. A metallurgical approach to metal contact dermatitis. Contact dermatitis 39, 213–221.

Goodman, J.E., Prueitt, R.L., Dodge, D.G., Thakali, S., 2009. Carcinogenicity assessment of water-soluble nickel compounds. Crit. Rev. Toxicol. 39, 365–417.

Goodman, J.E., Prueitt, R.L., Thakali, S., Oller, A.R., 2011. The nickel ion bioavailability model of the carcinogenic potential of nickel-containing substances in the lung. Crit. Rev. Toxicol. 41, 142–174.

Greenwood, N.N., Earnshaw, A., 1997. Chemistry of the elements. Pergamon Press plc.

Hamel, S.C., Buckley, B., Lioy, P.J., 1998. Bioaccessibility of metals in soils for different liquid to solid ratios in synthetic gastric fluid. Environ. Sci. Technol. 32, 358–362.

Hedberg, Y., Gustafsson, J., Karlsson, H.L., Möller, L., Odnevall Wallinder, I., 2010a. Bioaccessibility, bioavailability and toxicity of commercially relevant iron- and chromium-based particles: in vitro studies with an inhalation perspective. Part. Fibre Toxicol. 7, 23.

Hedberg, Y., Midander, K., Odnevall Wallinder, I., 2010b. Particles, sweat, and tears: a comparative study on bioaccessibility of ferrochromium alloy and stainless steel particles, the pure metals and their metal oxides, in simulated skin and eye contact. Integr. Environ. Assess. Manage. 6, 456–468.

Hedberg, Y., Hedberg, J., Liu, Y., Odnevall Wallinder, I., 2011. Complexation- and ligand-induced metal release from 316L particles: importance of particle size and crystallographic structure. Biometals 24, 1099–1114.

Henderson, R.G., Cappellini, D., Seilkop, S., Bates, H., Oller, A., 2012. Oral Bioaccessibility Testing and Read-Across Hazard Assessment of Nickel Compounds. Regul. Toxicol. Pharm. 63, 20–28.

Herting, G., Odnevall Wallinder, I., Leygraf, C., 2006. Factors that influence the release of metals from stainless steels exposed to physiological media. Corros. Sci. 48, 2120–2132.

Herting, G., Odnevall Wallinder, I., Leygraf, C., 2008. Metal release rate from AISI 316L stainless steel and pure Fe, Cr and Ni into a synthetic biological medium- a comparison. J. Environ. Monitor. 10, 1092–1098.

Horie, M., Nishio, K., Fujita, K., Kato, H., Nakamura, A., Kinugasa, S., Endoh, S., Miyauchi, A., Yamamoto, K., Murayama, H., Niki, E., Iwahashi, H., Yoshida, Y., Nakanishi, J., 2009. Ultrafine NiO particles induce cytotoxicity in vitro by cellular uptake and subsequent Ni(II) release. Chem. Res. Toxicol. 22, 1415–1426.

Hostynek, J.J., Dreher, F., Pelosi, A., Anigbogu, A., Maibach, H.I., 2001. Human stratum corneum penetration by nickel. Acta Derm.-Venereol. Suppl. 212, 5–10.

Huggins, F., Galbreath, K., Eylands, K., Loon, L.V., Olson, J., Zillioux, E., Ward, S., Lynch, P., Chu, P., 2011. Determination of nickel species in stack emissions from eight residual oil-fired utility steam-generating units. Environ. Sci. Technol. 45, 6188–6195.

Julien, C., Esperanza, P., Bruno, M., Alleman, L.Y., 2011. Development of an in vitro method to estimate lung bioaccessibility of metals from atmospheric particles. J. Environ. Monitor. 13, 621–630.

Kasprzak, K.S., Sunderman Jr, F.W., Salnikow, K., 2003. Nickel carcinogenesis. Mutat. Res., Fundam. Mol. Mech. Mutagen. 533, 67–97.

Kim, K.S., Winograd, N., 1974. X-ray photoelectron spectroscopic studies of nickel-oxygen surfaces using oxygen and argon ion-bombardment. Surf. Sci. 43, 625–643.

Kitakatsu, N., Maurice, V., Hinnen, C., Marcus, P., 1998. Surface hydroxylation and local structure of NiO thin films formed on Ni(111). Surf. Sci. 407, 36–58.

Kodama, Y., Ishimatsu, S., Matsuno, K., Tanaka, I., Tsuchiya, K., 1985. Pulmonary deposition and clearance of a nickel oxide aerosol by inhalation. Biol. Trace Elem. Res. 7, 1–9.

Kodama, Y., Tanaka, I., Matsuno, K., Ishimatsu, S., Kawamoto, T., 1993. Comparative deposition and clearance of various nickel compounds exposed by inhalation in rats. Biol. Trace Elem. Res. 36, 257–269.

Kuehn, K., Sunderman, F.W., 1982. Dissolution half-times of nickel compounds in water, rat serum, and renal cytosol. J. Inorg. Biochem. 17, 29–39.

Lidén, C., Carter, S., 2001. Nickel release from coins. Contact Dermatitis 44, 160–165.
Lidén, C., Skare, L., Vahter, M., 2008. Release of nickel from coins and deposition onto skin from coin handling – comparing euro coins and SEK. Contact Dermatitis 59, 31–37.
Ludwig, C., Casey, W.H., 1996. On the mechanisms of dissolution of Bunsenite [NiO(s)] and other simple oxide minerals. J. Colloid Interf. Sci. 178, 176–185.
Ludwig, C., Devidal, J.-L., Casey, W.H., 1996. The effect of different functional groups on the ligand-promoted dissolution of NiO and other oxide minerals. Geochim. Cosmochim. Acta 60, 213–224.
MacDougall, B., Graham, M.J. (Eds.), 1995. Growth and Stability of Passive Films. Marcel Dekker, Inc., Paris, France (Chapter 5).
Marshakov, I.K., 2002. Anodic dissolution and selective corrosion of Alloys. Prot. Met. 38, 118–123.
McIntyre, N.S., Cook, M.G., 1975. X-ray photoelectron studies on some oxides and hydroxides of cobalt, nickel, and copper. Anal. Chem. 47, 2208–2213.
Menné, T., Calvin, G., 1993. Concentration threshold of non-occluded nickel exposure in nickel-sensitive individuals and controls with and without surfactant. Contact Dermatitis 29, 180–184.
Midander, K., Pan, J., Leygraf, C., 2006. Elaboration of a test method for the study of metal release from stainless steel particles in artificial biological media. Corros. Sci. 48, 2855–2866.
Midander, K., Pan, J., Odnevall Wallinder, I., Heim, K., Leygraf, C., 2007. Nickel release from nickel particles in artificial sweat. Contact Dermatitis 56, 325–330.
Midander, K., de Frutos, A., Hedberg, Y., Darrie, G., Odnevall Wallinder, I., 2010. Bioaccessibility studies of ferro-chromium alloy particles for a simulated inhalation scenario: a comparative study with the pure metals and stainless steel. Integr. Environ. Assess. Manage. 6, 441–455.
Mitchell, D.F., Sewell, P.B., Cohen, M., 1976. A kinetic study of the initial oxidation of the Ni(001) surface by RHEED and x-ray emission. Surf. Sci. 61, 355–376.
Miura, T., Patierno, S.R., Sakuramoto, T., Landolph, J.R., 1989. Morphological and neoplastic transformation of C3H/10T1/2 Cl 8 mouse embryo cells by insoluble carcinogenic nickel compounds. Environ. Mol. Mutagen. 14, 65–78.
Muñoz, A., Costa, M., 2012. Elucidating the mechanisms of nickel compound uptake: a review of particulate and nano-nickel endocytosis and toxicity. Toxicol. Appl. Pharmacol. 260, 1–16.
National Toxicology Program (NTP), 1996. Toxicology and carcinogenesis studies of Nickel Oxide (CAS No. 1313–99-1) in F344/N rats and B6C3F1 mice (inhalation studies). Bethesda MD: U.S. DHHS. NTP Technical ReportTR 451. NIH, Publication No. 96–3367.
Nyborg, L., Norell, M., Olefjord, I., 1992. Surface studies of powder metallurgical stainless steel. Surf. Interface Anal. 19, 607–614.
O'Brien, P., Salacinski, H.J., 1996. Evidence for a relationship between the generation of reactive intermediates and the physicochemical characteristics of nickel oxides. Arch. Toxicol. 70, 787–800.
Oller, A.R., Costa, M., Oberdörster, G., 1997. Carcinogenicity assessment of selected nickel compounds. Toxicol. Appl. Pharmacol. 143, 152–166.
Oller, A.R., Kirkpatrick, D.T., Radovsky, A., Bates, H.K., 2008. Inhalation carcinogenicity study with nickel metal powder in Wistar rats. Toxicol. Appl. Pharmacol. 233, 262–275.
Oller, A.R., Cappellini, D., Henderson, R.G., Bates, H.K., 2009. Comparison of nickel release in solutions used for the identification of water-soluble nickel exposures and in synthetic lung fluids. J. Environ. Monit. 11, 823–829.
Pedersen, L.K., Johansen, J.D., Held, E., Agner, T., 2004. Augmentation of skin response by exposure to a combination of allergens and irritants – a review. Contact Dermatitis 50, 265–273.
Pietruska, J.R., Liu, X., Smith, A., McNeil, K., Weston, P., Zhitkovich, A., Hurt, R., Kane, A.B., 2011. Bioavailability, intracellular mobilization of nickel, and HIF-1α activation in human lung epithelial cells exposed to metallic nickel and nickel oxide nanoparticles. Toxicol. Sci. 124, 138–148.
Skeaff, J., Adams, W.J., Rodriguez, P., Brouwers, T., Waeterschoot, H., 2011. Advances in metals classification under the United Nations globally harmonized system of classification and labeling. Integr. Environ. Assess. Manage. 7, 559–576.
Stumm, W., Morgan, J.J., 1996. Aquatic Chemistry: Chemical Equilibria and Rates in Natural Waters. John Wiley and Sons, New York.
Sunderman, F.W., Oskarsson, A., 1991. II.22 Nickel. In: Ernest, M. (Ed.), Metals and Their Compounds in the Environment - Occurence, Analysis and Biological Relevance. VCH, Weinheim, Germany.
Sunderman, F.W., Hopfer, S.M., Knight, J.A., McCully, K.S., Cecutti, A.G., Thornhill, P.G., Conway, K., Miller, C., Patierno, S.R., Costa, M., 1987. Physicochemical characteristics and biological effects of nickel oxides. Carcinogenesis 8, 305–313.
Takahashi, S., Oishi, M., Takeda, E., Kubota, Y., Kikuchi, T., Furuya, K., 1999. Physicochemical characteristics and toxicity of nickel oxide particles calcined at different temperatures. Biol. Trace Elem. Res. 69, 161–174.
Tanaka, I., Ishimatsu, S., Matsuno, K., Kodama, Y., Tsuchiya, K., 1986. Retention of nickel oxide (green) aerosol in rat lungs by long-term inhalation. Biol. Trace Elem. Res. 9, 187–195.
Turner, A., 2011. Oral bioaccessibility of trace metals in household dust: a review. Environ. Geochem. Health 33, 331–341.
Ullmann, Y., 2008. Elaboration of a Metal Release Test for Massive Metal Sheet – Effects of Different Parameters on the Copper Release Rate. Division Corrosion Science, KTH, Stockholm.
UN, 2009. The Globally Harmonized System of Classification and Labelling of Chemicals, Annex 10, Guidance on transformation/dissolution of metals and metal compounds in aqueous media.
Yamada, M., Takahashi, S., Sato, H., Kondo, T., Kikuchi, T., Furuya, K., Tanaka, I., 1993. Solubility of nickel oxide particles in various solutions and rat alveolar macrophages. Biol. Trace Elem. Res. 36, 89–98.